Nanomechanics of cellulose deformation reveal molecular defects that facilitate natural deconstruction

Peter N. Ciesielski[a,1], Ryan Wagner[b], Vivek S. Bharadwaj[a], Jason Killgore[b], Ashutosh Mittal[a], Gregg T. Beckham[c], Stephen R. Decker[a], Michael E. Himmel[a], and Michael F. Crowley[a,1]

[a]Biosciences Center, National Renewable Energy Laboratory, Golden, CO 80401; [b]Material Measurement Laboratory, National Institute of Standards and Technology, Boulder, CO; and [c]National Bioenergy Center, National Renewable Energy Laboratory, Golden, CO 80401

Edited by Alexis T. Bell, University of California, Berkeley, CA, and approved April 2, 2019 (received for review January 4, 2019)

Technologies surrounding utilization of cellulosic materials have been integral to human society for millennia. In many materials, controlled introduction of defects provides a means to tailor properties, introduce reactivity, and modulate functionality for various applications. The importance of defects in defining the behavior of cellulose is becoming increasingly recognized. However, fully exploiting defects in cellulose to benefit biobased materials and conversion applications will require an improved understanding of the mechanisms of defect induction and corresponding molecular-level consequences. We have identified a fundamental relationship between the macromolecular structure and mechanical behavior of cellulose nanofibrils whereby molecular defects may be induced when the fibrils are subjected to bending stress exceeding a certain threshold. By nanomanipulation, imaging, and molecular modeling, we demonstrate that cellulose nanofibrils tend to form kink defects in response to bending stress, and that these macromolecular features are often accompanied by breakages in the glucan chains. Direct observation of deformed cellulose fibrils following partial enzymatic digestion reveals that processive cellulases exploit these defects as initiation sites for hydrolysis. Collectively, our findings provide a refined understanding of the interplay between the structure, mechanics, and reactivity of cellulose assemblies.

cellulose | cellulases | atomic force microscopy | molecular dynamics | quantum mechanics

Cellulose is an abundant biopolymer that is naturally mass-produced on a global scale and is closely tied to life on earth in many ways throughout the biosphere. Technology surrounding utilization of cellulosic materials will be a central component of the transition to a sustainable bioeconomy (1, 2). The vast majority of cellulose originates from biosynthesis of plant cell walls (3) wherein they provide structural reinforcement to an impressive biopolymer assembly that has inspired modern fiber-reinforced nanocomposite materials (4). Advances in cellulose processing have led to promising technologies such as cellulosic biofuels (5) and advanced biobased materials (6). Efforts to optimize processes that convert cellulosic feedstocks to fuels and chemicals have demonstrated that integrating mechanical disruption with chemical and enzymatic deconstruction can dramatically enhance yields (7–10). Production of cellulosic nanomaterials also relies heavily on mechanical refining methods. Ruminant animals, which are indeed successful at utilizing cellulosic biomass as source of carbon and energy, employ extensive mastication to ease digestion and thereby offer additional lessons from Nature regarding the effectiveness of mechanical disruption for cellulose conversion purposes (11). The enhancement of biomass conversion processes by mechanical disruption has thus far been largely attributed to macroscale phenomena such as particle size reduction; and nano-to-mesoscale phenomena, such as cell wall delamination and nanofibrillation, which facilitate access of cellulose fibrils to enzymes and chemical catalysts (12–15). Some insightful studies have also shown that mechanically induced deformations of whole pulp fibers, termed "dislocations," are preferentially degraded by acid (16) and enzymatic hydrolysis (17). In 2011 Thygesen et al. (18) offered the first direct evidence that endoglucanase enzymes bind selectively to dislocations in whole fiber cells and articulated the importance of this phenomenon in the context of cellulosic biofuel production. This work was followed by additional studies that further demonstrated the potential of dislocations to introduce reactivity in processes that convert cellulose into soluble sugars for production of biofuels and biochemicals (19–21). However, these studies that have investigated dislocations at the scale of whole fiber cells provide little insight into molecular and macromolecular phenomena which are the focus of the present work. To differentiate dislocations (i.e., regions of lignocellulose fibers that exhibit a different organization of the cellulose microfibrils) from the molecular features investigated in the present work, we chose to use the term "defect" which is commonly employed by the materials science community to describe alterations in the local molecular organization of polymers.

Kink dislocations in cellulose assemblies have been theoretically depicted for over 70 y beginning in 1946 by Dadswell and Wardrop (22), and later in 1972 by the work of Rowland and Roberts (23). The authors postulated that these kinked locations are associated with so-called "amorphous" regions of cellulose which are more susceptible to acid hydrolysis but offered no direct evidence to substantiate their hypothesis. Many publications have since presented schematics of cellulose fibrils depicting alternating crystalline and amorphous domains to explain the formation of relatively uniform cellulosic fragments, termed cellulose nanocrystals, produced

Significance

Cellulose plays an important role as a structural polymer for natural material applications and as a source of sugars for production of renewable fuels and chemicals. Previously, kink defects have been observed in isolated cellulose nanofibrils. In this work, we provide direct evidence that these defects can be induced by mechanical deformation and are often accompanied by molecular-level bond breakages that are exploited by cellulase enzymes as initiation sites for processive hydrolysis. This relationship between mechanical stress and molecular defect formation has likely played a role in the evolution of both plants and natural cellulolytic enzyme systems. An improved understanding of these principles provides insight for the development of advanced cellulose utilization and processing technologies.

Author contributions: P.N.C., J.K., G.T.B., M.E.H., and M.F.C. designed research; P.N.C., R.W., V.S.B., J.K., A.M., S.R.D., and M.F.C. performed research; P.N.C., R.W., V.S.B., J.K., A.M., S.R.D., and M.F.C. analyzed data; and P.N.C., R.W., V.S.B., J.K., A.M., G.T.B., S.R.D., M.E.H., and M.F.C. wrote the paper.

The authors declare no conflict of interest.

This article is a PNAS Direct Submission.

This open access article is distributed under Creative Commons Attribution-NonCommercial-NoDerivatives License 4.0 (CC BY-NC-ND).

[1]To whom correspondence may be addressed. Email: Peter.Ciesielski@nrel.gov or michael.crowley@nrel.gov.

This article contains supporting information online at www.pnas.org/lookup/suppl/doi:10.1073/pnas.1900161116/-/DCSupplemental.

Published online April 29, 2019.

by controlled hydrolysis of cellulosic substrates (8, 24, 25). However, the origins (26), structural interpretation (27), and even presence of such periodic crystalline and amorphous domains of cellulose in native cell walls remain topics of debate among researchers (28). Obvious kinked regions are clearly observable in many published micrographs of isolated cellulose nanofibrils (29, 30). Recently, Usov and coworkers published a detailed, imaging-based study of cellulose kinks in 2,2,6,6-tetramethylpiperidine 1-oxyl radical (TEMPO)-oxidized nanofibrils, and concluded that the non-Gaussian distribution of kink angles is inconsistent with the canonical concept of alternating amorphous and crystalline regions (3). This observation implies that the presence and locations of kink defects are not necessarily intrinsic properties of cellulose fibrils, but rather they are induced when fibrils are subjected to certain externally applied conditions. Still, absent from the previous literature has been a rigorous, molecular-level understanding of mechanically induced defects in cellulose, as well as direct evidence of their implications for ubiquitous processes such as enzymatic deconstruction for biofuel and nanomaterial production.

Results

Mechanical Induction of Defects by Direct Nanomanipulation. The response of cellulose nanofibrils to externally applied mechanical stress was characterized by direct manipulation of single nanofibrils by atomic force microscopy (AFM). Initial nanomanipulation was performed by translating the AFM tip in a straight line across the silicon substrate surface against a cellulose fibril. Manipulation resulted in multiple distinct responses in the cellulose. AFM images shown in Fig. 1 *A*–*C*″ taken before and after a series of nanomanipulation trajectories illustrate characteristic responses. Complete sequences of manipulations are shown in *SI Appendix*, Figs. S1 and S2. Typically, the first manipulation trajectory does not cross the entirety of the fiber and serves to loosen the cellulose fiber from the substrate, allowing less-constrained modification in subsequent steps. Fig. 1 *A*–*A*″ presents an example of mechanically induced kink formation at and adjacent to the tip–fibril contact point. Initial shallow kink angles are further bent with additional loading to ∼90°. With insufficient mobility of the fibril on the substrate due to adhesion, tip trajectories can also cut or break the fiber near the contact point, as is observed in Fig. 1 *B*–*B*″. Notably, the breakage does not occur at the previous kink location in this example. These complete breakages clearly show that covalent bonds may be broken by mechanical deformation. However, large kinking angles alone are insufficient to cause complete breakage during all nanomanipulation experiments. To confirm that the apparent kinks (such as in Fig. 1*A*) are not a result of complete breaks, trajectories that place a kinked segment in tension were used to straighten kinks. Fig. 1 *C*–*C*″ demonstrates that multiple kinks can be completely straightened with no lingering topographic artifacts, showing structural connectivity of the fibril was maintained after kinking. These observations imply that the formation of kink defects result from rearrangements of glucan chains within the fibril that do not necessarily break all covalent bonds within the glucan chains. This hypothesis is consistent with the observations of Thygesen et al. (31), who showed that cellulose chains may continue unbroken through dislocations observed at the scale of whole fiber cells. However, without molecular-scale resolution at the kink location, we are unable to determine by AFM topography data alone whether kink formation results in local irreparable covalent modifications to the nanofibrils that may be superficially straightened, or reversible reconfigurations of the hydrogen bonds.

Nanomanipulation on substrate-bound cellulose is effective to establish that individual fibrils can be kinked by mechanical forces, but it does not allow for straightforward quantification of the kinking forces or stresses. To measure the forces associated

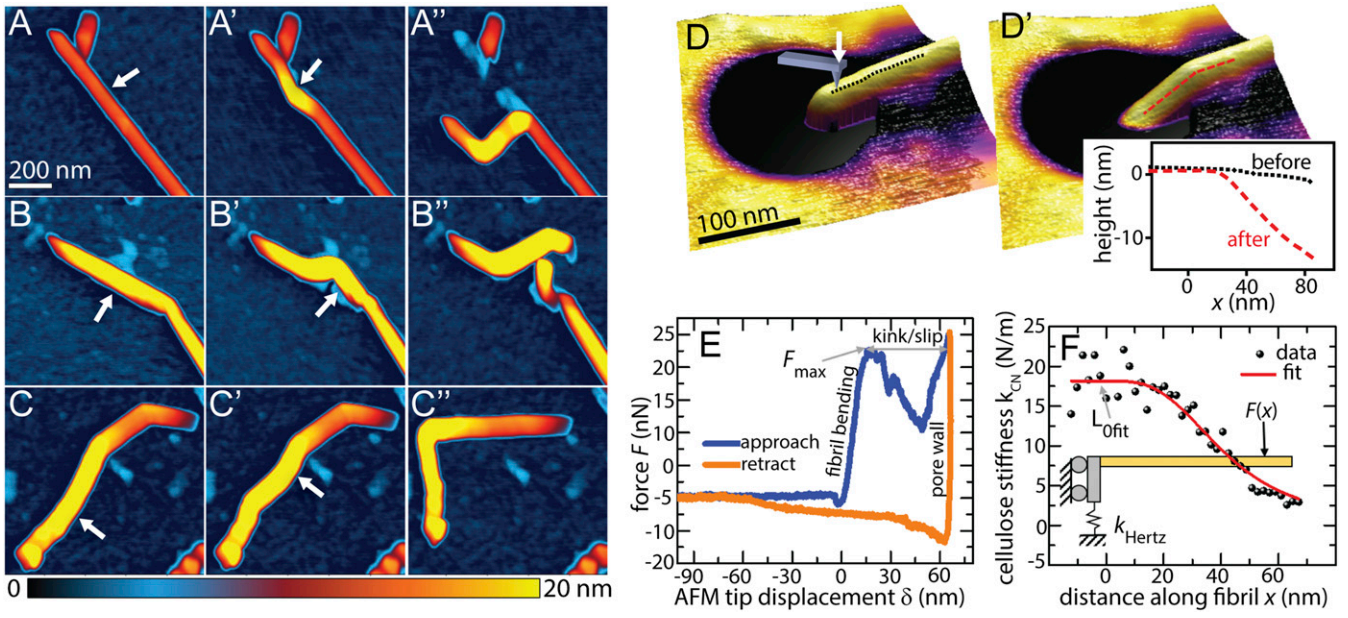

Fig. 1. Probing mechanical deformation at the nanoscale reveals reversible and irreversible nature of cellulose kinks. (*A*–*D*′) AFM images of cellulose nanofibrils before and after a series of lithographic lateral manipulations with the AFM tip demonstrate three typical responses. The arrow in each image indicates the location and direction of applied force. (*A*–*A*″) Multiple kinks were induced along the length of the fibril. (*B*–*B*″) Complete breakage of the fibril was achieved by applying manipulation to the vicinity of an existing kink defect, while the fibril was strongly adhered to the substrate. (*C*–*C*″) A previously kinked fibril was straightened, indicating that the kinks observed in *C* and *C*′ still maintain some degree of molecular connectivity. (*D*) A cellulose nanofibril suspended over a 200-nm pore in track-etched polycarbonate (TEPC). (*D*′) Kink defect formed in the same nanofibril shown in *D* after AFM indentation at 48-nN applied load. (*Inset*) Comparison of the topographic line profile of the nanofibril before and after indentation, clearly revealing the presence of a mechanically induced kink at the supporting pore wall. (*E*) Approach and retract indentation curves for the particular indentation step that induced kinking in the nanofibril. After reaching the maximum force F_{max} in the approach curve the cellulose forms a kink, allowing the probe tip to slip into the pore wall. (*F*) AFM indentation and bending measurements along the length of a nanofibril were fit to a beam model to calculate deformation stress.

with nanofibril deformation, force-versus-displacement (F-Z) measurements were performed on cellulose fibrils suspended over pores in track-etched polycarbonate (TEPC). An example of this configuration is shown in Fig. 1*D*. As observed with the substrate-bound fibrils, boundary constraints played a key role in the nature of the mechanical deformation. For suspended structures, kinked configurations such as that shown in Fig. 1*D′* were most readily achieved by pushing downward on cellulose fibrils that were single-cantilevered (rather than double-cantilevered) over pores because the unconstrained end allowed the freedom of movement required to accommodate the kinked geometry. In total, kinking was observed on eight of the investigated single-cantilevered fibrils. Kinking forces ranging from 24 to 47 nN were identified from the F-Z curve (details are included in *SI Appendix*), as shown for a representative fibril in Fig. 1*E* and *SI Appendix*, Fig. S4. A series of F-Z measurements was also performed at forces below the kinking threshold to allow fitting to an elastic Euler–Bernoulli beam model, as shown in Fig. 1*F*. Of the eight kinked fibrils, two datasets exhibited sufficient goodness of fit to the model to calculate deformation stresses of (4.0 ± 1.4) GPa and (3.2 ± 1.1) GPa (details are included in *SI Appendix*). These stress values are close to the theoretical tensile yield stress of cellulose (8), which indicates that significant covalent bond failure at the fibril surface likely contributes to the onset of kink formation. The kinking stresses and forces further provide useful criteria for the design of mechanical processes that maximize kink formation in cellulosic materials for various processing scenarios.

Molecular Simulations of Mechanical Deformation and Glycosidic Bond Breakage. Deformation of cellulose nanofibrils was investigated in silico to provide molecular-level insight into mechanically induced defect formation. Previously, we reported the propensity of atomic models of cellulose nanofibrils to form kinks to accommodate externally imposed curvature (32). This topic has since been investigated by molecular-dynamics (MD) simulation by Chen et al. (33). However, neither of the aforementioned studies incorporated bond breakages that may occur as glucan chains within the fibril are strained by severe bending, and thereby neglected a potentially important aspect of a fibril's response to mechanical deformation. Several studies have investigated bond breakage in the context of linear strain, wherein reactive MD was performed by comparing bonding topologies to a quantum-mechanics (QM)-based parameter set at frequent time steps (34, 35). While these studies of linear strain focused on a potentially important failure mechanism of cellulose fibrils, they did not elucidate relationships between strain and longer-range structural transitions or demonstrate changes to the chemical or biochemical reactivity of the nanofibrils.

In the present work, we develop a more holistic computational approach to investigate macromolecular deformation coupled to bond breaking, wherein a pseudo reactive MD method accounts for strain-induced glycosidic bond breakage without requiring a computationally demanding reactive bond order potential. A distance criterion that characterizes glycosidic bond breakage under strain was derived from QM calculations on a representative model system. The bond-breakage event occurs when the force that the bond can withstand is exceeded. The force at which this occurs is identified as the maximum of the first derivative of the quantum energy plotted as the black line in Fig. 2*A*. The glycosidic linkage distance at which this force is attained in an MD simulation, shown as the blue line in Fig. 2*A*, is chosen as the MD distance criterion for breaking the linkage. Every glycosidic distance is evaluated during MD simulation at regular intervals and is broken when it is found to exceed the breaking distance criterion. The main computational studies were performed using 36-chain fibril models with a two-point bending geometric configuration similar to the experiment shown in Fig. 1 *D* and *D′*. The response to mechanical stress was modeled with a series of simulations, each at constant force applied to the end of the cellulose bringing it to equilibrium under the applied load. At regular intervals, glycosidic bonds exceeding the breaking criterion were replaced by hydrolyzed glucan chain ends and the chains were relaxed to remove accumulated strain before continuing the simulation at the next applied force interval. Additional details regarding these simulations are included in *SI Appendix*.

An example of the progression of mechanical deformation and associated strain-induced glycosidic bond breakage as predicted by the pseudoreactive MD simulation method is visualized in Fig. 2 *B–E*. The colormap used in this figure visualizes the similarity of the local atomic positions to that of the I-β crystal polymorph. Gray-colored regions indicate a highly ordered atomic structure, whereas red coloration indicates relatively disordered regions. Snapshots of the entire model shown in Fig. 2 *B–E* indicate that curvature is concentrated to a localized region rather than distributed throughout the length of the fibril. The associated coloration indicates that this concentrated curvature is accompanied by large departure from the I-β structure. As deflection increases in response to applied force, glycosidic chains begin to break initially on the outside surface of the curved region as visualized by red-orange spheres. In general, these computational results indicate that kink defects form as a result of the concentration of bending stresses into localized regions. This acts to reduce the curvature of adjacent segments and lower the energy of the fibril ensemble, which is consistent with previous computational studies of this phenomenon (32, 33). The angle of bending and number of broken bonds predicted by the simulation is plotted as a function of applied force in Fig. 2*F*. Trends in both of these quantities with increasing force indicate two distinct regimes of nanofibril deformation. Both increase linearly as the applied load is increased up to ∼3.5 nN, beyond which the rates of progression in bond breakage and angle of bending increase significantly. We attribute the increase in deformation to a combination of two phenomena. Firstly, the departure from structural energy minimum of the I-β polymorph is concentrated into the proximity of the bend to maintain the majority of the fibril in a nonbent configuration. This occurrence leads to the formation of the "kinked" structure, and subsequent deformation is accommodated by this local disordered region with minimal disruption to the molecular order of the remainder of the fibril. Secondly, breakage of a significant number of covalent bonds also facilitates increased deformation rates, which in turn results in more bond breakages. These predictions are well-aligned with the findings of Thygesen and Gierlinger (38), who used Raman microspectroscopy to observe a less-ordered molecular structure of cellulose in the vicinity of dislocations at the scale of whole hemp fibers.

Digestion with Cellobiohydrolase Results in Local Sharpening at Kink Defects. Isolated cellulose fibrils were incubated with purified cellulase enzyme to investigate possible relationships between enzymatic activity and observable macromolecular defects (i.e., kinks) in cellulose nanofibrils. Several processive cellulases from the *Trichoderma reesei* Glycoside Hydrolase (GH) Family 6 and 7 cellobiohydrolases (termed GH Cel6A and Cel7A, respectively) have been extensively characterized and exhibit well-known, highly specific digestion mechanisms (39). Cel7A initiates hydrolysis at the free reducing ends of glucan chains and proceeds unidirectionally along the chain with each hydrolytic event. Similarly, Cel6A initiates hydrolysis at nonreducing ends and proceeds unidirectionally as hydrolysis occurs, thereby exhibiting processivity in the opposite direction of Cel7A with respect to the glucan chain (40). These degradation mechanisms have been shown to result in readily observable morphological features of partially digested cellulose fibrils. Specifically, digestion by Cel7A results in a "sharpening" or tapering effect of the reducing ends of cellulose fibrils (41), whereas digestion by Cel6A results in selective sharpening of nonreducing ends (42).

Isolated *Cladophora* cellulose fibrils were incubated with a preparation of purified Cel7A enzyme and the morphologies of the cellulose fibrils were investigated before and after enzymatic

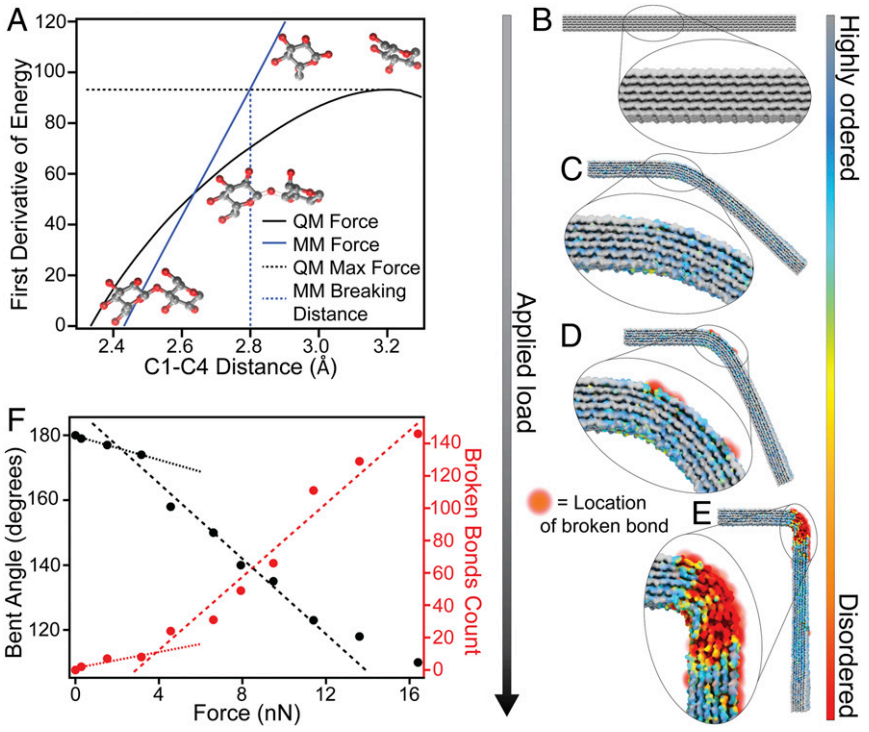

Fig. 2. Atomistic simulations -predict significant bond breakages occur when deformation reaches a critical threshold. (*A*) Derivation of the distance criterion for bond breaking in cellulose. Bond breakage is characterized by the maximum on the QM force curve (black). The bond-breaking distance criterion for MD is defined as the C1–C4 distance at which the molecular mechanics force (blue) matches the maximum QM force. (*B–E*) Snapshots from the pseudoreactive MD simulation showing the structural progression of a cellulose nanofibril subjected to increasing load in a two-point bend configuration. (*F*) Trends in both the bent angle and number of broken bonds with increasing force indicate distinct regimes of deformation and bond breakage. The substantial increase in rates of bending and bond breakage are attributed to localized departure from the stable 1-β structure in tandem with broken covalent bonds, both of which act to reduce the mechanical integrity of the fibril at the location of the deformation. The models used in these simulations were constructed in the I-β polymorph (36, 37) comprising 36 glucan chains with degree of polymerization 100.

hydrolysis by transmission electron microscopy (TEM). Details of these experiments and imaging methods are included in *SI Appendix*. TEM images showing several examples of kink defect sites in *Cladophora* fibrils before and after partial digestion by Cel7A are presented in Fig. 3 *A–C* and Fig. 3 *D–F*, respectively. Before digestion, kink defects were commonly observed; however, these features were not accompanied by localized narrowing of the fibrils. Following digestion, most kink defects were accompanied by an obvious localized, tapered geometry as exemplified in Fig. 3 *D–F*. Measurements of the thicknesses of the fibrils on either side of the kink defect reveal that one side was preferentially sharpened, which we attributed to the selective, unidirectional processivity of Cel7A (41). These results provide strong support for our computational predictions that extreme kink defects introduce breakages in the glucan chains, which then provide initiation sites for hydrolysis by processive hydrolytic enzymes.

Discussion

The relationship between the nanoscale geometry and molecular structure elucidated by these results suggests the origin of the commonly depicted concept of cellulose fibrils with alternating crystalline and amorphous domains. More specifically, our results refine and extend the hypotheses regarding the presence of concentrated, stress-induced disorder in cellulose originally offered by Rowland and Roberts (23) over four decades ago. Glucan chains accommodating curvature along the length of the fibril experience a departure from the thermodynamically favorable configuration associated with the cellulose I-α and I-β polymorphs. In response, cellulose fibrils tend to concentrate extreme curvature into localized regions to minimize curvature over the majority of length of the fibril. This results in relatively small regions of molecular disorder, which we postulate have been historically identified as amorphous domains; similarly, longer, relatively straight regions with a higher degree of molecular organization were likely historically interpreted as the "crystalline" domains. The concentration of disorder into small localized regions in response to mechanical stress may be why changes in crystallinity resulting from mechanical processing are nearly undetectable when measured using ensemble techniques such as by X-ray diffraction and NMR (15). Additionally, these findings are consistent with the results presented by Thygesen et al. (18), who demonstrated that cellulose in the vicinity of dislocations largely retains a crystalline orientation sufficient to produce birefringence observable by polarized light microscopy. The aforementioned study also demonstrated preferential binding of endoglucanase enzymes to dislocations observed at the scale of whole pulp fibers. Endoglucanase enzymes do not require free glucan chain ends to initiate hydrolysis but have been known to prefer disordered cellulose over more crystalline substrates (39). The highly localized regions of molecular disorder that accompany kink defects as predicted by our simulations may provide favorable locations for endoglucanase binding; however, our results do not offer experimental evidence of this hypothesis which should be the topic of future investigations. Furthermore, multiscale studies of cellulase interactions with dislocations and molecular defects should be undertaken to determine how behavior observed at the scale of whole fiber cells may translate to interactions between enzymes and individual nanofibrils.

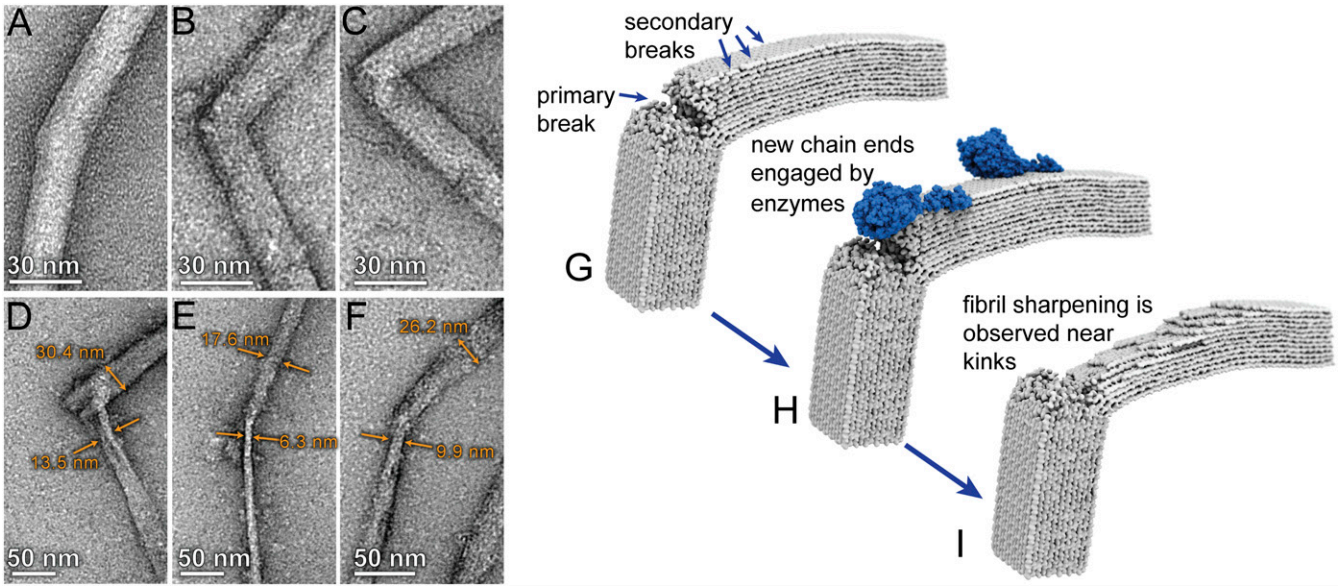

Fig. 3. Imaging of cellulose nanofibrils before and after enzymatic hydrolysis shows that Cel7A preferentially initiates hydrolysis at the location of kink defects: (*A*–*C*) TEM micrographs showing examples of kink defects in isolated *Cladophora* cellulose nanofibrils. (*D*–*F*) After incubation with purified Cel7A, the nanofibrils exhibited localized narrowing in close proximity to the kink defect. Measurements of fibril width indicate that narrowing is more severe on one side of the defect. (*G*–*I*) Schematic depiction of the proposed mechanism for localized hydrolysis at kink defects by the processive cellobiohydrolase Cel7A, wherein reducing ends formed by bond breakages at the kink location (*G*) are engaged by the enzyme (*H*). Unidirectional hydrolysis results in formation of additional reducing ends on the same side of the kink defect, which are subsequently engaged by additional enzymes. This process results in preferential narrowing of the fibril on one side of the defect as enzymatic digestion progresses (*I*).

Even newly synthesized cellulose fibrils in plant cell walls exhibit directional changes when continuous fibrils are observed over lengths greater than 1 μm and kinks are present where extreme curvature is apparent (43), which likely contributes to the amorphous content of cellulose reported to be present in intact plant cell walls (44). Similarly, studies of dislocations at the scale of whole fiber cells have shown that they persist even in plants in the complete absence of mechanical stresses other than those associated with natural growth (45). These observations suggest that periodic occurrences of molecular disorder are not necessarily an inherent property of cellulose, but rather a result of the geometric configurations that the fibril was subjected to during biosynthesis and/or postprocessing. This interpretation is also consistent with the well-known "leveling off of degree of polymerization" that is encountered during acid hydrolysis of cellulose (46), in that kink defects, and associated regions of molecular disorder that are preferentially degraded during acid hydrolysis, will not form with a spatial frequency exceeding that allowed by the persistence length of the cellulose fibril (3). Additional support for this concept was offered by a study that demonstrated that the fiber size evolution during agitated enzymatic hydrolysis could be well-described by a simple, yet insightful, simulation that employed a three-point bending model with a breaking moment that was continually weakened due to hydrolysis (47).

In the context of cellulose metabolism in the biosphere, it is not surprising that cellulose-digesting organisms have evolved enzymes that take advantage of these naturally occurring defects. This reasoning also suggests incentives for cellulolytic organisms to evolve endoglucanases (48) and lytic polysaccharide monooxygenases (49) to introduce molecular defects in polysaccharides that improve performance of the processive cellobiohydrolases. Organisms that emerged as the most successful metabolizers of lignocellulose, such as ruminants and some insects, augment enzymatic digestion with mechanical maceration which likely provides advantages beyond simple particle-size reduction in light of the findings presented here. Cellulose evolved to function as a material with long-term stability in Nature; however, hidden within relationships between its hierarchical structure and mechanical behavior are solutions to its deconstruction which enable biological exploitation of molecular defects.

Optimization of mechanical defect induction to improve enzymatic hydrolysis processes is indeed a complex undertaking. A recent study that investigated the relationship between mechanical agitation and enzymatic hydrolysis efficacy clearly demonstrated that conventional mixing can drive agglomeration of biomass and thereby reduce the substrate surface area accessible to enzymes (50). In the context of the present work and other aforementioned studies that obviate the molecular and macromolecular advantages of mechanical energy input to improve hydrolysis yields, we suggest that reactor hydrodynamics, comminution, and agitation mechanisms be cooptimized for next-generation saccharification systems.

Conclusions

We have provided evidence that macromolecular kink defects in cellulose nanofibrils provide localized initiation sites for enzymatic hydrolysis. By direct nanomanipulation of individual cellulose nanofibrils in an AFM, we confirm that kink defects may be induced by mechanical deformation. We used pseudoreactive MD simulation to further support the hypothesis that formation of kink defects is commonly accompanied by strain-induced glyosidic bond breakages, which serve as initiation sites for hydrolysis by cellobiohydrolase enzymes. These molecular- and macromolecular-level insights into the formation and characteristics of defects in cellulose provide a refined understanding of the fundamental structure and behavior of cellulose nanofibrils and provide additional insight regarding the origin of the previously reported benefits of mechanical refining for cellulose conversion processes. Furthermore, these results suggest opportunities for the development of improved cellulose processing paradigms that exploit systematic, nanomechanical defect induction to tune the materials properties of the resultant cellulose and improve its reactivity in conversion scenarios.

Methods

Detailed description of the materials and methods involved in the preparation of cellulose nanofibrils, AFM, TEM, Cel7A production and purification, enzymatic hydrolysis, and molecular simulations are provided in *SI Appendix*.

ACKNOWLEDGMENTS. This work was authored by Alliance for Sustainable Energy, LLC, the manager and operator of the National Renewable Energy Laboratory for the US Department of Energy (DOE) under Contract DE-AC36-08GO28308. Funding provided by the Center for Direct Catalytic Conversion of Biomass to Biofuels (C3Bio), an Energy Frontier Research Center funded by the US DOE, Office of Science, Office of Basic Energy Sciences, Award DE-SC0000997.

1. Fitzgerald ND (2017) Chemistry challenges to enable a sustainable bioeconomy. *Nat Rev Chem* 1:0080.
2. Zhu H, et al. (2016) Wood-derived materials for green electronics, biological devices, and energy applications. *Chem Rev* 116:9305–9374.
3. Bomble YJ, et al. (2017) Lignocellulose deconstruction in the biosphere. *Curr Opin Chem Biol* 41:61–70.
4. Ling S, Kaplan DL, Buehler MJ (2018) Nanofibrils in nature and materials engineering. *Nat Rev Mater* 3:18016.
5. Ragauskas AJ, et al. (2006) The path forward for biofuels and biomaterials. *Science* 311:484–489.
6. Moon RJ, Martini A, Nairn J, Simonsen J, Youngblood J (2011) Cellulose nanomaterials review: Structure, properties and nanocomposites. *Chem Soc Rev* 40:3941–3994.
7. Chen X, et al. (2016) DMR (deacetylation and mechanical refining) processing of corn stover achieves high monomeric sugar concentrations (230 g L− 1) during enzymatic hydrolysis and high ethanol concentrations (> 10% v/v) during fermentation without hydrolysate purification or concentration. *Energy Environ Sci* 9:1237–1245.
8. Wang W, et al. (2014) Effect of mechanical disruption on the effectiveness of three reactors used for dilute acid pretreatment of corn stover Part 1: Chemical and physical substrate analysis. *Biotechnol Biofuels* 7:57.
9. Kelsey RG, Shafizadeh F (1980) Enhancement of cellulose accessibility and enzymatic hydrolysis by simultaneous wet milling. *Biotechnol Bioeng* 22:1025–1036.
10. Paye JMD, et al. (2016) Biological lignocellulose solubilization: Comparative evaluation of biocatalysts and enhancement via cotreatment. *Biotechnol Biofuels* 9:8.
11. Weimer PJ, Russell JB, Muck RE (2009) Lessons from the cow: What the ruminant animal can teach us about consolidated bioprocessing of cellulosic biomass. *Bioresour Technol* 100:5323–5331.
12. Mosier N, et al. (2005) Features of promising technologies for pretreatment of lignocellulosic biomass. *Bioresour Technol* 96:673–686.
13. Ciesielski PN, et al. (2014) Effect of mechanical disruption on the effectiveness of three reactors used for dilute acid pretreatment of corn stover Part 2: Morphological and structural substrate analysis. *Biotechnol Biofuels* 7:47.
14. Jeoh T, et al. (2007) Cellulase digestibility of pretreated biomass is limited by cellulose accessibility. *Biotechnol Bioeng* 98:112–122.
15. de Assis T, et al. (2018) Toward an understanding of the increase in enzymatic hydrolysis by mechanical refining. *Biotechnol Biofuels* 11:289.
16. Stone J (1961) The influence of wood damage on pulp quality. *Tappi J* 44:166A–175A.
17. Ander P, Hildén L, Daniel G (2008) Cleavage of softwood kraft pulp fibres by HCl and cellulases. *BioResources* 3:477–490.
18. Thygesen LG, Hidayat BJ, Johansen KS, Felby C (2011) Role of supramolecular cellulose structures in enzymatic hydrolysis of plant cell walls. *J Ind Microbiol Biotechnol* 38: 975–983.
19. Usov I, et al. (2015) Understanding nanocellulose chirality and structure-properties relationship at the single fibril level. *Nat Commun* 6:7564.
20. Molnár G, et al. (2018) Cellulose crystals plastify by localized shear. *Proc Natl Acad Sci USA* 115:7260–7265.
21. Hidayat BJ, Felby C, Johansen KS, Thygesen LG (2012) Cellulose is not just cellulose: A review of dislocations as reactive sites in the enzymatic hydrolysis of cellulose microfibrils. *Cellulose* 19:1481–1493.
22. Dadswell HE, Wardrop AB (1946) Cell wall deformations in wood fibres. *Nature* 158: 174–175.
23. Rowland SP, Roberts EJ (1972) Nature of accessible surfaces in the microstructure of cotton cellulose. *J Polym Sci A Polym Chem* 10:2447–2461.
24. Salas C, Nypelö T, Rodriguez-Abreu C, Carrillo C, Rojas OJ (2014) Nanocellulose properties and applications in colloids and interfaces. *Curr Opin Colloid Interface Sci* 19:383–396.
25. Mariano M, El Kissi N, Dufresne A (2014) Cellulose nanocrystals and related nanocomposites: Review of some properties and challenges. *J Polym Sci B Polym Phys* 52: 791–806.
26. McFarlane HE, Döring A, Persson S (2014) The cell biology of cellulose synthesis. *Annu Rev Plant Biol* 65:69–94.
27. Nam S, French AD, Condon BD, Concha M (2016) Segal crystallinity index revisited by the simulation of X-ray diffraction patterns of cotton cellulose Iβ and cellulose II. *Carbohydr Polym* 135:1–9.
28. Agarwal UP, Ralph SA, Reiner RS, Baez C (2016) Probing crystallinity of never-dried wood cellulose with Raman spectroscopy. *Cellulose* 23:125–144.
29. Elazzouzi-Hafraoui S, et al. (2008) The shape and size distribution of crystalline nanoparticles prepared by acid hydrolysis of native cellulose. *Biomacromolecules* 9: 57–65.
30. Kaushik M, Fraschini C, Chauve G, Putaux J-L, Moores A (2015) Transmission electron microscopy for the characterization of cellulose nanocrystals. *The Transmission Electron Microscope Theory and Applications*, ed Maaz K (IntechOpen, London), pp 129–163.
31. Thygesen LG, Bilde-Sørensen JB, Hoffmeyer P (2006) Visualisation of dislocations in hemp fibres: A comparison between scanning electron microscopy (SEM) and polarized light microscopy (PLM). *Ind Crops Prod* 24:181–185.
32. Ciesielski PN, et al. (2013) 3D electron tomography of pretreated biomass informs atomic modeling of cellulose microfibrils. *ACS Nano* 7:8011–8019.
33. Chen P, Ogawa Y, Nishiyama Y, Ismail AE, Mazeau K (2016) Linear, non-linear and plastic bending deformation of cellulose nanocrystals. *Phys Chem Chem Phys* 18: 19880–19887.
34. Wu X, Moon RJ, Martini A (2014) Tensile strength of Iβ crystalline cellulose predicted by molecular dynamics simulation. *Cellulose* 21:2233–2245.
35. Wu X, Moon RJ, Martini A (2013) Crystalline cellulose elastic modulus predicted by atomistic models of uniform deformation and nanoscale indentation. *Cellulose* 20: 43–55.
36. Nishiyama Y, Langan P, Chanzy H (2002) Crystal structure and hydrogen-bonding system in cellulose Ibeta from synchrotron X-ray and neutron fiber diffraction. *J Am Chem Soc* 124:9074–9082.
37. Matthews JF, et al. (2006) Computer simulation studies of microcrystalline cellulose Ibeta. *Carbohydr Res* 341:138–152.
38. Thygesen LG, Gierlinger N (2013) The molecular structure within dislocations in Cannabis sativa fibres studied by polarised Raman microspectroscopy. *J Struct Biol* 182:219–225.
39. Payne CM, et al. (2015) Fungal cellulases. *Chem Rev* 115:1308–1448.
40. Igarashi K, et al. (2011) Traffic jams reduce hydrolytic efficiency of cellulase on cellulose surface. *Science* 333:1279–1282.
41. Imai T, Boisset C, Samejima M, Igarashi K, Sugiyama J (1998) Unidirectional processive action of cellobiohydrolase Cel7A on Valonia cellulose microcrystals. *FEBS Lett* 432: 113–116.
42. Chanzy H, Henrissat B (1985) Undirectional degradation of Valonia cellulose microcrystals subjected to cellulase action. *FEBS Lett* 184:285–288.
43. Zhang T, Mahgsoudy-Louyeh S, Tittmann B, Cosgrove DJ (2014) Visualization of the nanoscale pattern of recently-deposited cellulose microfibrils and matrix materials in never-dried primary walls of the onion epidermis. *Cellulose* 21:853–862.
44. Thygesen A, Oddershede J, Lilholt H, Thomsen AB, Ståhl K (2005) On the determination of crystallinity and cellulose content in plant fibres. *Cellulose* 12:563–576.
45. Thygesen LG, Asgharipour MR (2008) The effects of growth and storage conditions on dislocations in hemp fibres. *J Mater Sci* 43:3670–3673.
46. Nelson ML, Tripp VW (1953) Determination of the leveling-off degree of polymerization of cotton and rayon. *J Polym Sci* 10:577–586.
47. Thygesen LG, Thybring EE, Johansen KS, Felby C (2014) The mechanisms of plant cell wall deconstruction during enzymatic hydrolysis. *PLoS One* 9:e108313.
48. Beldman G, Voragen AG, Rombouts FM, Pilnik W (1988) Synergism in cellulose hydrolysis by endoglucanases and exoglucanases purified from Trichoderma viride. *Biotechnol Bioeng* 31:173–178.
49. Vaaje-Kolstad G, et al. (2010) An oxidative enzyme boosting the enzymatic conversion of recalcitrant polysaccharides. *Science* 330:219–222.
50. Digaitis R, Thybring EE, Thygesen LG (November 23, 2018) Investigating the role of mechanics in lignocellulosic biomass degradation during hydrolysis. *Biotechnol Prog*, 10.1002/btpr.2754.